CHARACTERIZATION OF TRIPLE-LAYER PHOSWICH DETECTOR FOR RADIOXENON MEASUREMENTS

Abi T. Farsoni and David M. Hamby

Oregon State University

Sponsored by the National Nuclear Security Administration

Contract No. DE-FC52-06NA27322
Proposal No. BAA06-36

ABSTRACT

Monitoring the atmosphere for xenon radioisotopes is one of the routines used to confirm a nuclear weapons test. The International Monitoring System (IMS) has been established to install and employ radioxenon detectors in various locations to verify nuclear weapons tests around the world. A beta/gamma coincidence spectroscopy technique has been shown to be the best measurement solution for monitoring ultra-low concentrations of radioxenons. The majority of radioxenon detection systems, such as the Automated Radioxenon Sampler and Analyzer (ARSA), use separate detectors to capture beta/gamma coincident events. In the ARSA detector, to detect one beta/gamma coincidence event, anode signals from six photomultiplier tubes must be collected and analyzed. Additionally, to reduce the memory effect, four identical gas cells are employed on a rotational basis to provide continuous monitoring. This therefore involves 12 photomultiplier tubes (PMTs) in one detection unit, making it a complex system that is difficult to calibrate. To simplify the coincidence detection setup, a phoswich detector can be used in which beta/gamma coincidence events are detected using one single photomultiplier tube.

We have developed a phoswich detector with three scintillation layers. The first layer is a thin plastic scintillator to detect beta and conversion electrons. The second layer is a CaF_2 scintillator which is intended for x-ray (30 keV) detection. And, a NaI(Tl) scintillator is used as the third layer for gamma ray detection. Coincident events are discriminated from single events, including background radiations, using digital pulse shape analysis. In this paper we discuss several characteristics of our system, including: (1) background measurements, (2) energy resolution, (3) the ability of our innovative digital pulse shape processing technique in discriminating beta-only, gamma-only and gamma-beta coincidence events, (4) energy calibration procedure and (5) results from our recent measurements with commercially available ^{133}Xe.

OBJECTIVE

A major element of the IMS network is monitoring xenon radioisotope releases from nuclear explosions. To detect ultra-low radioxenon, several detection systems, such as ARSA and SAUNA, have been developed and are currently under test. These systems detect radioactive xenon by employing separate detectors to measure beta-gamma coincidence events in their gas cell, facilitating background rejection. The beta-gamma coincidence technique makes these systems very sensitive to the four xenon radioisotopes ^{131m}Xe, ^{133m}Xe, ^{133}Xe and ^{135}Xe (McIntyre et al., 2001 and 2006). Using this technique, a 2D beta-gamma spectrum is updated only when the beta and gamma detectors are triggered within a predetermined time. Because of employing 12 PMTs in the ARSA system, such a complex system can easily become out-of-calibration after a long counting run.

Phoswich detectors have recently been considered as an alternative to simplify radioxenon detection (Ely et al., 2003; Hennig et al., 2005; Farsoni et al., 2008). In a phoswich detector, two or more scintillation layers are coupled to a single PMT. The energy deposition in each layer from incident beta and/or gamma, in coincidence or singles, is then determined via digital pulse shape analysis of the PMT's anode pulses.

A two-channel phoswich detector has been designed specifically for radioxenon detection (Farsoni et al., 2007). The detector consists of a thin hollow disk (2 mm thickness and 76.2 mm diameter) as the xenon gas cell, surrounded by two identical planar triple-layer phoswich detectors. In designing the detector, several priorities have been considered, including improving the 30-keV x-ray/(CE + beta) coincidence region, increasing the system sensitivity by employing both dual and triple coincidence counting, improving light collecting uniformity, and decreasing the overall cost by simplifying the detector design. To digitally capture the PMT's anode pulses from the two phoswich detectors, a two-channel high-performance digital pulse processor (250 MSPS, 12 bits per channel) was designed and constructed. We also developed a graphical user interface (GUI) for controlling the digital processor, detecting coincidence events and reconstructing 2D coincidence beta/gamma spectra (Farsoni et al., 2008).

A prototype and full-scale triple-layer phoswich detector has been constructed to characterize one half of the final detection system. In this paper we discuss several characteristics of our system, including (1) background measurements, (2) energy resolution, (3) the ability of our innovative, digital, pulse-shape-processing technique to discriminate between beta-only, gamma-only and gamma-beta coincidence events, (4) energy calibration procedure, and (5) results from our recent measurements with commercially available ^{133}Xe.

RESEARCH ACCOMPLISHED

Prototype Phoswich Detector

A prototype phoswich detector with three scintillation layers has been constructed (Figure 1). The first layer is a thin plastic scintillator (1.5 mm) to detect beta and conversion electrons. The thickness of BC-400 is sufficient to absorb the vast majority of beta/CE particles emitted from radioxenons. The second layer is a CaF_2 scintillator (2.0 mm), which is intended for x-ray (30 keV) detection. The third layer is a NaI(Tl) scintillator (25.4 mm) to detect high-energy gamma-rays. Since the NaI(Tl) is highly hygroscopic, this layer is isolated from other scintillators using a 6.35-mm quartz optical window.

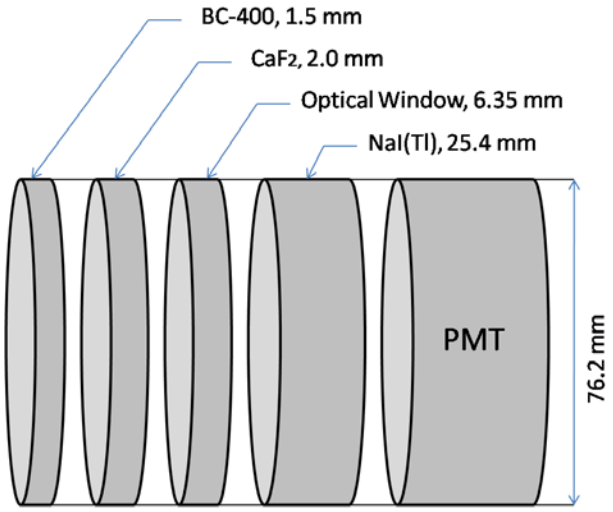

Figure 1. Schematic diagram of the prototype triple-layer phoswich detector.

Event Discrimination and Energy Measurement

Coincident events are discriminated from single events, including background radiations, using digital pulse shape analysis. Depending on how the incident radiation releases its energy within each layer of the phoswich detector, seven possible pulse shapes or types could be generated at the PMT's anode output. Using three digital triangular filters (Farsoni at al., 2008), the integration or sum of three areas (A, B, and C in Figure 2) of the anode pulse is calculated. These sums are used for pulse shape discrimination and energy measurement purposes.

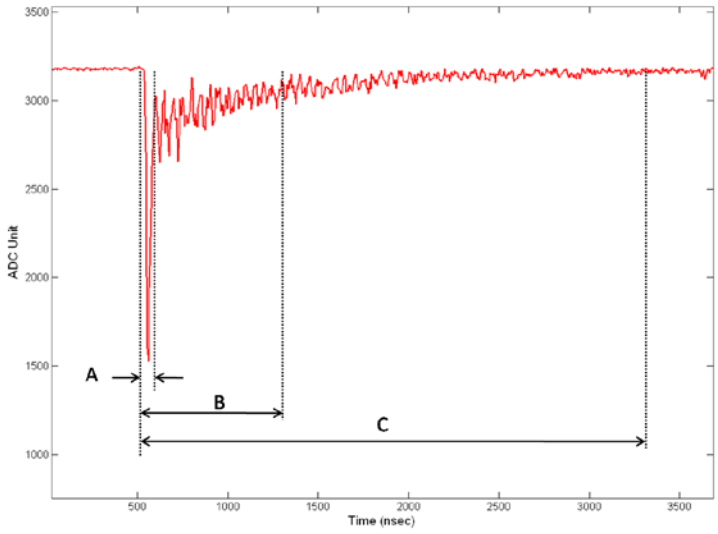

Figure 2. A typical phoswich pulse when a coincidence event has occurred in the detector. Three filter sums (A, B, and C) are used to discriminate different events and measure the energy released in each phoswich layer.

Using these sums, two ratios—fast component ratio (FCR) and slow component ratio (SCR)—are calculated from each captured pulse to discriminate different pulse shapes. The FCR and SCR range from zero to unity.

Figure 3 shows a 2D scatter plot of the FCR and SCR when the phoswich detector is exposed to a ^{137}Cs source. During this experiment, the ^{137}Cs source was shielded against beta and conversion electrons. Regions 1, 2 and 4 represent single events in plastic (BC-400), CaF_2 and NaI layers, respectively. Regions 3 and 5 show coincidence events of CaF_2-plastic and NaI-plastic, respectively. Regions 6 and 7 accommodate either Compton scattering events between NaI and CaF_2 or unknown events. Events in these regions have no useful information for our application and thus are rejected.

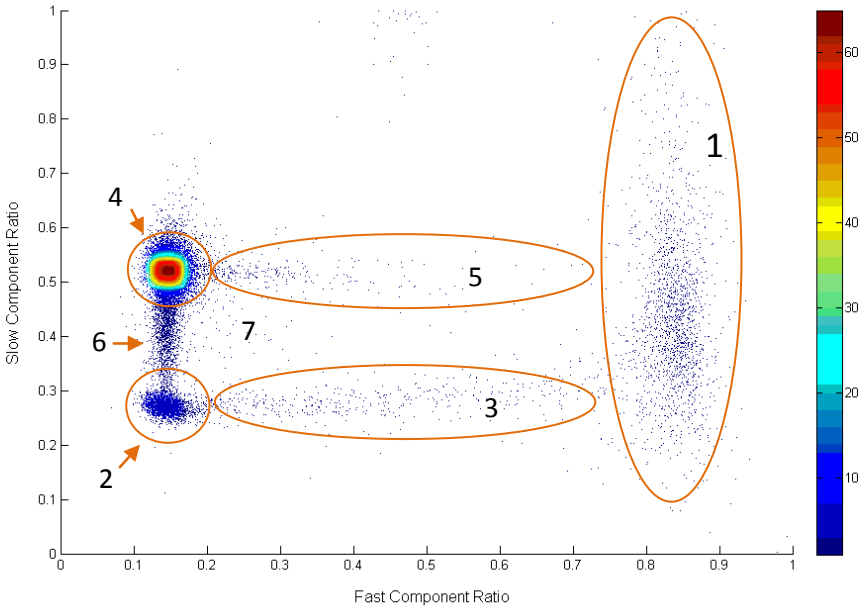

Figure 3. Scatter of fast and slow component ratios from ^{137}Cs. Seven marked regions correspond to seven pulse shapes, indicating how gamma rays interact with the three layers of phoswich detector.

Ideally, beta-only events from the plastic scintillator (Region 1) should be populated in a vertical distribution with an average FCR close to unity. Region 1 in Figure 3 has an average FCR of 0.84. To investigate possible reasons, beta-only events in Region 1 were carefully examined. Events in this region, as depicted in Figure 4, show a significant "ringing effect" following the fast decaying component of the plastic scintillator. The same results were observed from a pure beta emitter. We believe that this effect is responsible for underestimating the FCR of beta-only events in Region 1. This effect is also observed with coincidence events when a fast decaying component is followed by a slow component (Figure 2). A moving average filter was used to check the net response of this effect (blue waveform in magnified portion of Figure 4). The response of this filter shows a nonzero area under the baseline. Obviously, this introduces errors in both pulse-shape analysis and energy measurement. We found a linear relationship between the sum A and the net area due to a ringing effect under sums B and C when a fast pulse from the plastic scintillator appears at the anode output. From this analysis, two correction factors were obtained and applied to all pulse processing and energy calculations in this paper. The detector manufacturer confirmed that the detector's PMT (9305KFLB) has a low-quality voltage divider and that it is responsible for this effect. Two other phoswich detectors with high-quality PMTs have been ordered and will be characterized in the near future.

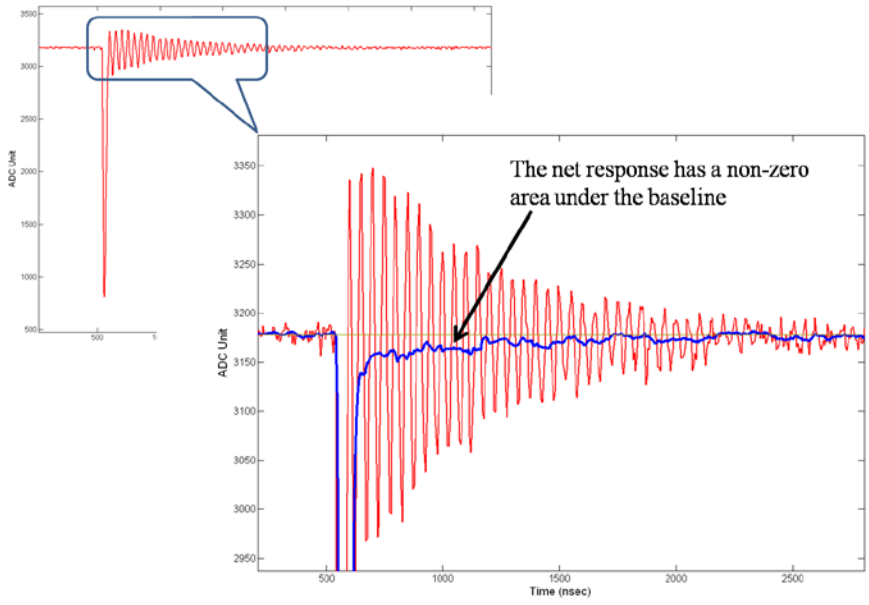

Figure 4. A fast pulse (after radiation absorption in plastic scintillator) is followed by a ringing effect. In the magnified portion, a moving average filter was used (blue waveform) to examine the average baseline level after the fast scintillation pulse.

Phoswich Detector Characterization

Background measurement

To measure the background count rate and investigate the system capability to discriminate different events, the phoswich detector was placed in a lead enclosure with a wall thickness of 2 in. The total background count rate from all events is 4.91 cps, of which 0.02 cps and 0.08 cps are coincidence events in NaI-plastic (Region 5) and CaF_2-plastic (Region 3), respectively. The total background count rate of the ARSA detector is ~30 cps, of which 0.1 cps is coincidence. The fraction of coincidence events in NaI-plastic is low (0.44%) but it is relatively high (1.72%) in CaF_2-plastic. We suspect that the ringing effect, mentioned before, mischaracterizes some events in the coincidence regions of 3 and 5, shown in Figure 3.

Energy calibration and resolution measurements

A ^{137}Cs source was used to calibrate three layers of the phoswich detector. Figure 5 depicts the 2D energy histogram from ^{137}Cs. Figure 5, left, shows the 2D energy histogram for the plastic (Ep) and CaF_2 (Ec) scintillators, whereas Figure 5, right, shows that of the plastic (Ep) and NaI (En) scintillators. Again, Regions 3 and 5 were used to reconstruct these histograms, respectively. In this measurement, the ^{137}Cs source was shielded against beta and conversion electrons to capture only gamma interactions with the phoswich layers. Since there is no beta coincidence with gamma rays, the 2D coincidence histograms shows only Compton scattering between layers. When a 662-keV gamma ray is scattered from one scintillator and is absorbed in the other scintillator, the total energy deposition should be equal to the original energy (662 keV). This forms a line of constant energy in the 2D histogram. Therefore, the intersections of black dashed lines with the corresponding energy axis in Figure 5, left, and Figure 5, right, were used to calibrate each layer.

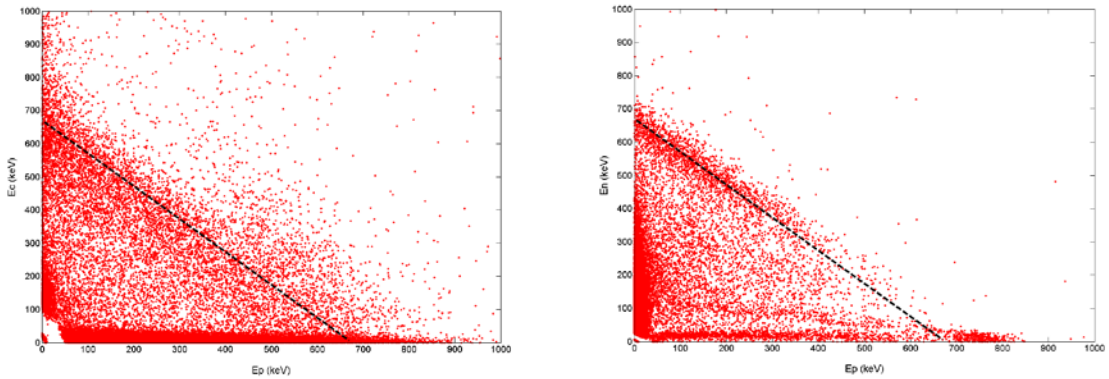

Figure 5. Two-dimensional energy histograms from a ^{137}Cs source. The one on the left is the 2D energy histogram for the plastic (Ep) and CaF_2 (Ec) scintillators, whereas the one on the right is that of the plastic (Ep) and NaI (En) scintillators.

Single events in Regions 2 and 4 of Figure 3 were used to reconstruct the NaI (blue) and CaF_2 (red) energy spectra (Figure 6). The NaI histogram shows all features of a healthy and typical spectrum from ^{137}Cs. Characteristic x-rays from ^{137m}Ba (30 keV) and lead shield (75 keV), backscatter peak, Compton edge and 662-keV photopeak are pronounced in the NaI spectrum. Because of a high-threshold setup for this experiment, only Compton scattering events can be seen in the CaF_2 spectrum. The measured resolution—full width by half maximum (FWHM)—for 662 keV of ^{137}Cs was 7.9%. The ARSA system has a resolution of 12% for 662-keV gamma rays (Reeder et al., 2004). NaI-only and CaF_2-only events have a fraction of 87.1% and 5.2% from all events, respectively. The fraction of coincidence events between these layers and plastic scintillator were 0.3% and 0.83%, respectively.

Two lab sources (^{109}Cd and ^{57}Co) were used to measure the energy resolution (FWHM) of 22-keV, 88-keV, and 122-keV x-rays and gamma rays. The energy resolution of 22 keV is 36%, which was measured from events in Region 2. Using the Region 4 in Figure 3, the energy resolution of 88 keV and 122 keV was 17% and 13.9%, respectively. The ARSA system has a resolution of 22% for 122-keV gamma rays (Reeder et al., 2004).

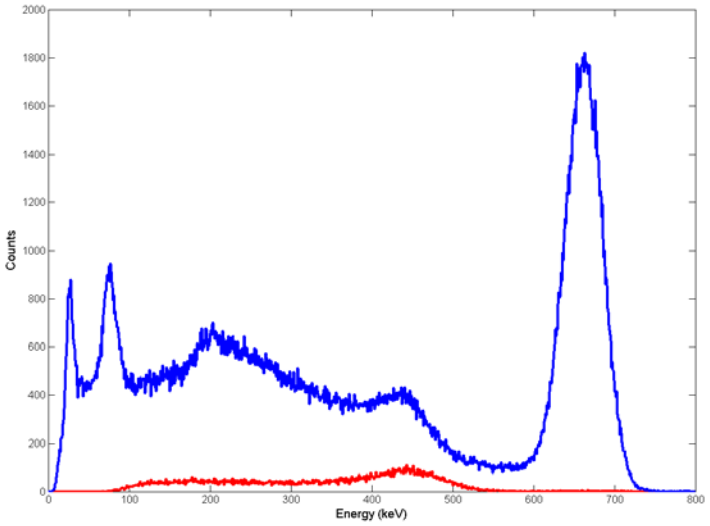

Figure 6. The ^{137}Cs spectra in NaI (blue) and CaF_2 (red), which were collected from events in Figure 3's Regions 4 and 2, respectively.

Radioxenon measurements

Commercially available ^{133}Xe gas was used to evaluate the capabilities of the phoswich detector and our digital pulse shape discrimination technique in radioxenon monitoring. Figure 7 shows 2D energy spectra from ^{133}Xe processed from Regions 3 and 5 of Figure 3, respectively. In both Figures, beta-gamma coincidence lines of 30-keV x-rays and 80-keV gamma rays from ^{133}Xe can be identified. As expected, the 30-keV x-rays are more pronounced in the CaF_2 coincidence spectrum, whereas the NaI coincidence spectrum shows higher efficiency for detection of the 80-keV gamma rays.

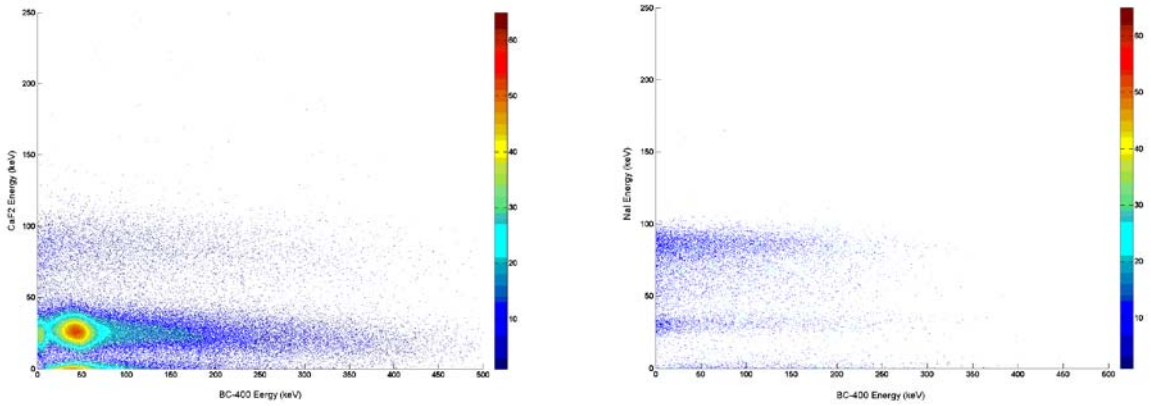

(a) (b)

Figure 7. Two-dimensional beta-gamma coincidence energy histograms from ^{133}Xe. As expected, the 30 keV x-rays are more pronounced in the CaF_2 coincidence energy spectrum (left), whereas the NaI coincidence spectrum (right) shows higher efficiency for detection of the 80 keV gamma rays.

Figure 8 shows energy histograms from the CaF_2 scintillator when the phoswich detector was exposed to ^{133}Xe. The red spectrum is reconstructed from events in Figure 3's Region 2 (CaF_2-only events). The blue spectrum is also from the CaF_2 layer, but when it is in coincidence with an event in the plastic scintillator (Region 3). The 30 keV and 80 keV peaks from ^{133}Xe can be seen in this figure. The energy resolution of 30 keV from the plastic-CaF_2 coincidence histogram was measured to be 43%. This value for ARSA detector (in NaI) is 32%. If we define the beta-gamma coincidence efficiency as the number of net coincidence counts in a region of interest (peak), divided by the number of all counts in that region (Hennig et al., 2007), the histograms in Figure 8 show a coincidence efficiency of 98.8% for detecting beta-gamma coincidence events in the 30-keV x-ray region of ^{133}Xe.

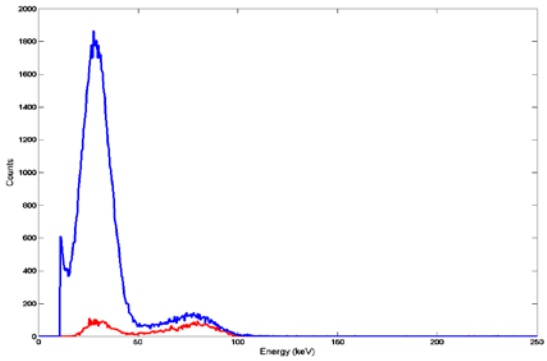

Figure 8. CaF_2 energy spectra from ^{133}Xe. Red and blue spectra were processed from events in Figure 3's Region 2 (CaF_2-only events) and Region 3 (BC400-CaF_2 coincidence events), respectively.

In Figure 9, energy histograms of the ^{133}Xe from the NaI(Tl) scintillator are shown. The red spectrum is reconstructed from events in Region 4 (NaI-only events) of Figure 3. The blue spectrum is also from NaI layer, but when it is in coincidence with events in the plastic scintillator (Region 5). Both 30-keV and 80-keV peaks from ^{133}Xe can be seen here with a higher efficiency for 80-keV gamma rays. The energy resolution of 80 keV from the plastic-NaI coincidence spectrum was measured to be 18%. The coincidence efficiency, as defined before, is 48.5% for detecting beta-gamma coincidence events in 80-keV gamma ray region of ^{133}Xe.

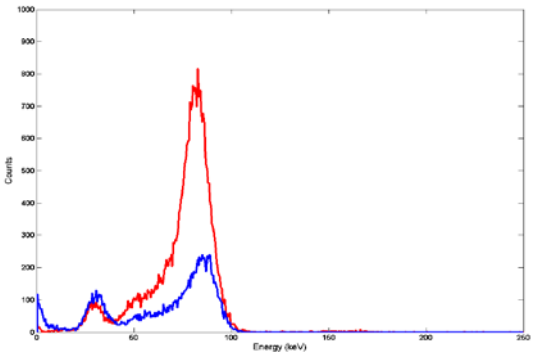

Figure 9. NaI(Tl) energy histograms from ^{133}Xe. Red and blue spectra were processed from events in Figrue 3's Region 4 (NaI-only events) and Region 5 (BC400-NaI coincidence events), respectively.

Beta energy histograms gated with two regions of interest in the gamma energy spectrum of ^{133}Xe, 30 keV and 80 keV, are shown in Figure 10. The blue histogram is processed from events in Region 3 (plastic-CaF_2 coincidence events) when a beta event from the plastic in coincidence with 30-keV x-ray from the CaF2 is detected. The 30-keV gated beta histogram shows a peak at 45 keV. This peak represents conversion electrons emitted in coincidence with 30-keV x-rays from ^{133}Xe. The energy resolution of this peak was measured to be 46%. This value was 50% in the ARSA system (Reeder et al., 2004). The red energy histogram in Figure 10 is reconstructed from events in Region 5 of Figure 3 (plastic-NaI coincidence events) when a beta event from the plastic is in coincidence with an 80-keV gamma ray from the NaI. The 80-keV gated beta energy histogram shows a beta continuum with no peak, as expected. Because of the possibility for triple-coincidence events in the 30-keV x-ray line from ^{133}Xe, where a beta particle and a 45-keV conversion electron can be coincidently deposited in the plastic scintillator, the endpoint of the 30-keV gated beta histogram (blue) is extended into higher energies (~400 keV).

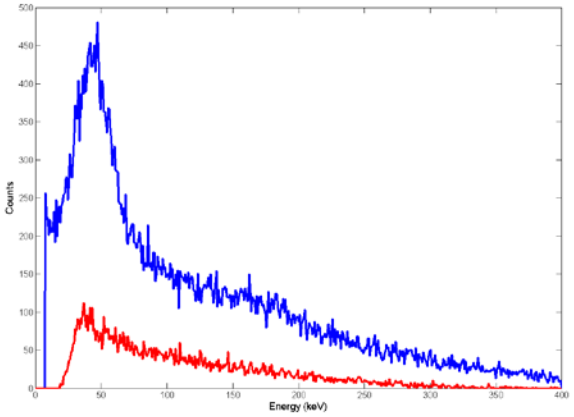

Figure 10. Beta energy histograms in plastic scintillator gated with (blue) 30-keV x-rays in CaF_2 and (red) 80-keV gamma ray in NaI. The 30-keV gated beta histogram shows a peak at 45 keV. This peak represents conversion electrons emitted in coincidence with 30-keV x-rays from ^{133}Xe.

As discussed earlier, the key characteristics of the current prototype phoswich detector and its digital pulse shape discrimination technique suffers from a ringing effect due to its low-quality PMT. Two new phoswich detectors with high performance PMTs are presently being constructed and will be characterized for radioxenon measurement in the near future.

CONCLUSION

We have characterized a triple-layer phoswich detector using radioactive lab sources and ^{133}Xe. The results provided in this paper demonstrate the ability of our innovative digital pulse shape processing technique to discriminate between beta-only, gamma-only, and gamma-beta coincidence events from a triple-layer phoswich detector. The phoswich detector shows a much lower background count rate than the ARSA detection system (4.91 cps vs. 30 cps). Compared with the ARSA system, in most gamma energy lines, we measured a better energy resolution. The energy resolution of the conversion electron peak at 45 keV from ^{133}Xe was measured to be 46%. This energy resolution is 50% in the ARSA system. Our measurements with this prototype phoswich detector show a coincidence efficiency of 98.8% and 48.5% for detecting beta-gamma coincidence events at 30-keV and 80-keV gamma lines of ^{133}Xe, respectively. Due to a low-quality PMT, a ringing effect appears following fast pulses from the plastic scintillator. This introduces errors in both pulse shape analysis and energy measurement. Although correction factors were applied to eliminate or reduce this effect, we believe that the overall performance of the phoswich detector and our digital pulse shape discrimination technique will be improved with a better PMT. Two new phoswich detectors with high-quality PMTs have been ordered and will be characterized for radioxenon measurement in the near future. These two detectors will form a two-channel phoswich detection system to detect and measure dual- and triple-coincidence events from xenon radioisotopes.

REFERENCES

Ely, J. H., C. E. Aalseth, J. C. Hayes, T. R. Heimbigner, J. I. McIntyre, H. S. Miley, M. E. Panisko, and M. Ripplinger (2003). Novel Beta-gamma coincidence measurements using phoswich detectors, in *Proceedings of the 25th Seismic Research Review – Nuclear Explosion Monitoring: Building the Knowledge Base*, LA-UR-03-6029, Vol. 2, pp. 533–541.

Farsoni, A. T., D. M. Hamby, K. D. Ropon, and S. E. Jones (2007). A two-channel phoswich detector for dual and triple coincidence measurements of radioxenon isotopes, in *Proceedings of the 29th Seismic Research Review: Ground-Based Nuclear Explosion Monitoring Technologies*, LA-UR-07-5613, Vol. 2, pp. 747–756.

Farsoni, A. T., D. M. Hamby, C. S. Lee, and A. J. Elliott (2008). Preliminary experiments with a triple-layer phoswich detector for radioxenon detection, in *Proceedings of the 30th Monitoring Research Review: Ground-Based Nuclear Explosion Monitoring Technologies*, LA-UR-08-05261, Vol. 2, pp. 739–748.

Hennig, W., H. Tan, W. K. Warburton, and J. I. McIntyre (2005). Digital pulse shape analysis with phoswich detectors to simplify coincidence measurements of radioactive xenon, in *Proceedings of the 27th Seismic Research Review: Ground-Based Nuclear Explosion Monitoring Technologies,* LA-UR-05-6407, Vol. 2, pp. 787–794.

Hennig, W., H. Tan, W. K. Warburton, A. Fallu-Labruyere, K. Sabourov, J. I. McIntyre, M. W. Cooper, and A. Gleyzer (2007). Characterization of phoswich well detectors for radioxenon monitoring, in *Proceedings of the 29th Monitoring Research Review: Nuclear Explosion Monitoring Technologies,* LA-UR-07-5613, Vol. 2, pp. 757–763.

McIntyre, J. I., K. H. Able, T. W. Bowyer, J. C. Hayes, T. R. Heimbigner, M. E. Panisko, P. L. Reeder, and R. C. Thompson (2001). Measurements of ambient radioxenon levels using the automated radioxenon sampler/analyzer (ARSA), *J. Radioanal. Nucl. Chem*. 248: 629–635.

McIntyre, J. I., T. W. Bowyer, and P. L. Reeder (March 2006). Calculation of minimum detectable concentration levels of radioxenon isotopes using the PNLL ARSA system, technical report, PNNL-13102.

Reeder, P. L., T. W. Bowyer, J. I. McIntyre, W. K. Pitts, A. Ringbom, and C. Johansson (2004). Gain calibration of coincidence spectrometer for automated radioxenon analysis, *Nucl. Instru. Methods Phys. Res., Sect. A* 521: 586–599.